

Structural and Bonding Behavior Analysis of Microwave Sintered ZnO:Co materials

D. Sivaganesh, S. Sasikumar, S. Saravanakumar, S. Asath Bahadur

Abstract— In this present study, $Zn_{1-x}Co_xO$ ($x = 0.0, 0.04$ & 0.06) samples were synthesized using conventional solid state sintering process and characterized by PXRD and SEM. The structural analysis was done using Rietveld profile refinement technique. The chemical bonding features and nature between Zn and O atoms was analyzed by charge distribution studies. The bonding between Zn and O is clearly visible in the three-dimensional and two-dimensional MEM maps. One-dimensional charge density distribution analysis clearly reveals that the characteristics of the bond. MEM results were also correlated with the PXRD parameters.

Keywords— X-ray diffraction, Rietveld Refinement, Scanning charge microscopy, Charge density distribution.

I. INTRODUCTION

In the past few decades, researchers have focused the transition metal oxides with great interest in various science and technological applications [1]. Among them, zinc oxide (ZnO) have paid enormous curiosity in the field of photocatalysis, electrocatalysis, catalysis, spintronics, optoelectronic devices, solar cells, energy storage devices and so forth owing to its peculiar properties including high photostability, superior chemical stability, good electrical conductivity and excellent exciton binding energy [2,3]. Due to its widespread applications, numerous researchers have been their attention for the synthesis of ZnO with various morphologies such as flower-like [4], rod-like [5], sphere-like [6], hexagonal structures [7] by various preparation routes, which includes solid states sintering [8], chemical methods [9-11], chemical vapor deposition [12] and ball milling methods [13] in order to improve their physical and chemical properties [4]. However, the aforesaid techniques have some limitations such as high temperature; high cost instruments and the obtained products were not uniform structures. Interestingly, microwave-assisted sintering (MWS) is an efficient route when compared to conventional

sintering [14]. Generally, conventional sintering could generate heat transfer by radiation or conduction and heat energy is transferred from the materials surface to the core by conduction. In contrast, during MWS process, the samples could catch the microwaves itself which provide the uniform particle growth with well-defined structures [15-17]. Generally, the electrons that present in the materials play a crucial role in conductivity, luminescence, and magnetic, insulating, semiconducting and piezoelectric properties. However, lack of reports available for the investigation charge density distributions in the Zn-O unit cell under microwave irradiation. Recently, our research group have been investigated the bonding nature and mid-bond charge densities of Al doped ZnO materials.

In this regard, we tried an attempt for the fabrication of Co^{2+} doped ZnO tailored via MWS route and characterized by XRD and SEM analysis. Also, we have evaluated the bonding nature and mid-bond charge densities of Co^{2+} doped ZnO.

II. EXPERIMENTAL

A. Sample preparation

The $Zn_{1-x}Co_xO$ ($x = 0.0, 0.04$ & 0.06) samples were synthesized using solid state sintering process. High purity starting materials ZnO (Alfa Aesar; purity: 99.99%) & Co_3O_4 (Alfa Aesar; purity: 99.98%) were added with stoichiometric molar ratio and ground using ball mill for 5 h. The mixture was transferred to quartz ampoules and then sintered at $1150^\circ C$ using microwave furnace. Then, the heated samples were cooled with at a rate of $50^\circ C$ per hour.

B. Characterization

$Zn_{1-x}Co_xO$ ($x = 0.0, 0.04$ & 0.06) samples were characterized by PXRD using monochromatic Bruker (D8 advance ECO) diffractometer with $CuK\alpha$ ($\lambda=1.54056 \text{ \AA}$) radiation from 10° to 120° with scan width of 0.02° . The detailed structural analysis was also done by Rietveld refinement technique. The microstructure and surface morphological images of the materials was measured using scanning electron microscopy (SEM) (ZEISS-EVO 18).

III. RESULTS AND DISCUSSION

A. Structural analysis

The crystalline purity of $Zn_{1-x}Co_xO$ ($x = 0.0, 0.04$ and 0.06) was determined by powder X-ray diffraction (PXRD) data sets.

Phase pure hexagonal



Revised Manuscript Received on July 22, 2019.

* Correspondence Author

S. Saravanakumar*, Department of Physics, International Research Centre, Kalasalingam Academy of Research and Education, Krishnankoil – 626126, Tamil Nadu, India. Email: saravanaphysics@gmail.com

D. Sivaganesh, Department of Physics, International Research Centre, Kalasalingam Academy of Research and Education, Krishnankoil – 626126, Tamil Nadu, India. Email: ganesh.siva650@gmail.com

S. Sasikumar, Department of Physics, International Research Centre, Kalasalingam Academy of Research and Education, Krishnankoil – 626126, Tamil Nadu, India. Email: sasikuhan@gmail.com

S. Asath Bahadur, Department of Physics, International Research Centre, Kalasalingam Academy of Research and Education, Krishnankoil – 626126, Tamil Nadu, India. Email: s_a_bahadur@yahoo.co.in

structured ZnO were identified and is compared to standard JCPDS patterns [18]. Fig. 1 shows the well-indexed observed PXRD profiles of the prepared Zn_{1-x}Co_xO (x = 0.0, 0.04 and 0.06) system. The intensity of diffraction peaks is gradual decrease with the addition of Co²⁺ concentration in ZnO. In general, the X-ray intensity of diffraction patterns depends only by the scattering factor of the atoms [19]. This is mainly caused by the atomic number of Zinc is 30 and the atomic number of Copper is 27. Due to the less atomic number of Co²⁺ the X- ray intensity of the peaks decreased gradually. On the other hand, the peaks shifted towards the lower side of 2θ for x=0.04 and peaks shifted to higher angle 2θ side for x = 0.06.

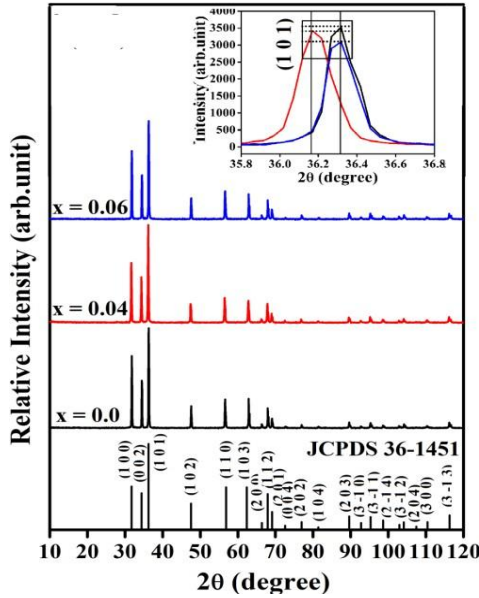
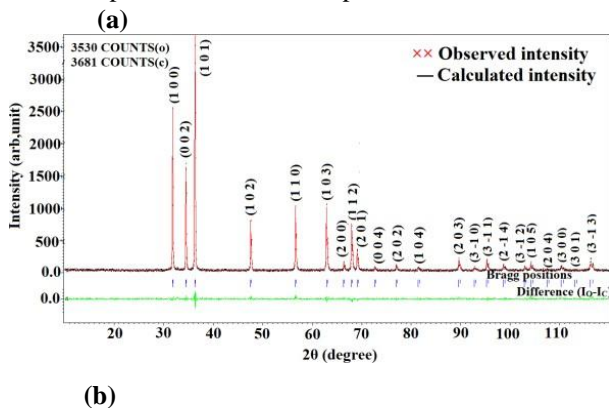


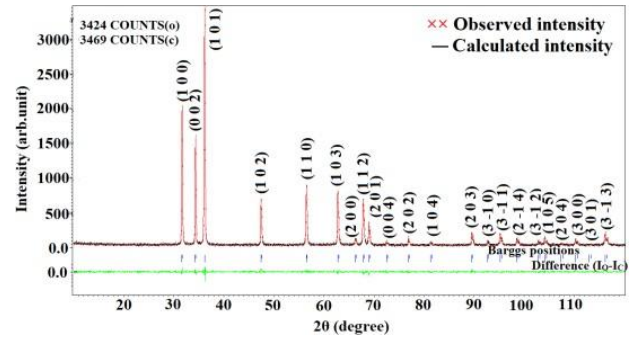
Fig. 1. PXRD patterns of Zn_{1-x}Co_xO materials (x=0.0, 0.04, 0.06).

These result consistent with the cell parameter shown in Table 1. The intensity variation and the peak shifting confirm that Cobalt ions occupied the ZnO substitutional lattice site. The crystallite size of the materials is calculated by Scherrer formula [20] and the size of Zn_{1-x}Co_xO (x = 0.0, 0.04 and 0.06) materials are 14 nm, 16 nm and 14 nm respectively.

The obtained XRD data sets of Zn_{1-x}Co_xO (x = 0.0, 0.04 and 0.06) samples were fitted using Rietveld refinement technique [21] by the software JANA 2006. The structure pattern was taken from wurtzite ZnO in space group of P63mc and both Zn and O at 2b Wyckoff positions, (1/3 2/3 0) and (1/3 2/3 0.375) respectively. The refined profile of Zn_{1-x}Co_xO (x = 0.0, 0.04 and 0.06) are depicted in fig. 2 (a)-(c). The refined cell parameters of the samples listed in table 1.



(b)



(c)

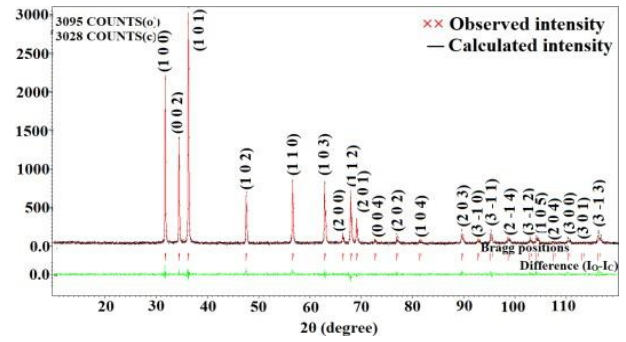


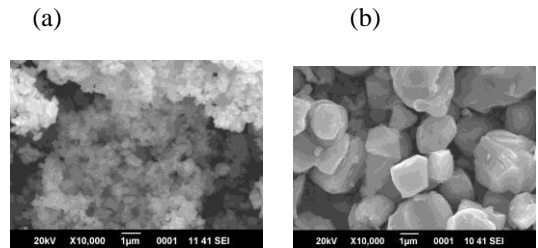
Fig. 2. Rietveld Refinement profiles of Zn_{1-x}Co_xO materials, a) x=0.0, b) x=0.04, c) x=0.06.

TABLE I. REFINED PARAMETERS OF THE PREPARED MATERIALS

Parameters	x=0	x=0.04	x=0.06
a=b (Å)	3.2511(9)	3.2546(13)	3.2438(42)
c (Å)	5.2049(16)	5.2113(21)	5.1927(68)
Volume (Å ³)	47.63(2)	47.80(3)	47.39(5)
Density (g/cm ³)	5.64	5.63	5.41
Robs(%) ^a	1.83	2.03	1.44
Rp(%) ^b	3.33	3.43	3.36
F ₍₀₀₀₎	76	74.64	73.96
GOF ^d	1.02	1.02	1.00

B. Microstructural studies

The microwave sintered Zn_{1-x}Co_xO (x = 0.0, 0.04 and 0.06) materials were evaluated by scanning electron microscopic images (SEM) to analyze the microstructure and surface morphological analysis and is shown in fig. 3 (a)-(c). There is an enormous change in the morphology of pure ZnO and Co²⁺ doped ZnO materials. Irregular hexagonal shaped morphology was observed in the pure ZnO and is shown in fig. 3(a). Fig. 3 (b) & (c) shows well dispersed and mine stone like morphology was observed. The approximate size of the particle is in the range of 1 μm.



(c)

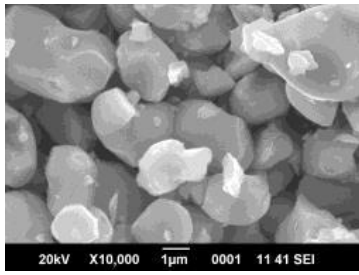


Fig. 3. SEM images of Zn_{1-x}Co_xO materials a) x=0.0, b) x=0.04, c) x=0.06.

C. Charge density analysis

The charge acquired characteristics were analyzed using the extracted structure factors. This analysis is done by maximum entropy method (MEM) [22] which is versatile software and standard method to analyze the charge density distribution inside unit cell employed by the DYSNOMIA software [23]. In this report, the charge density distributions inside unit cell is reconstructed for Zn_{1-x}Co_xO (x = 0.0, 0.04 and 0.06) samples. Three-dimensional, two-dimensional and one-dimensional charge density views can be visualized by VESTA software [24].

Fig. 4 (a)-(c) show the distributions charges inside the unit cell of Zn_{1-x}Co_xO (x = 0.0, 0.04 and 0.06) samples with iso-surface level 1 e/Å³. The Zinc and Oxygen atoms placed on the horizontal axis is referred by Bond 1 and the Zn-O bond along the vertical axis is mentioned by Bond 2 [17]. Fig. 5 and 6 show the two-dimensional charge density distributions drawn on (100) and (014) planes. Fig. 7 shows the bond length and charge density at the middle of the bonds which is evaluated by one-dimensional charge density profiles and the mid bond charge densities listed in table 2. It reveals that the mid-bond charge density values for 4% Co²⁺ doped ZnO material shows maximum value at Bond 1 and minimum value at Bond 2.

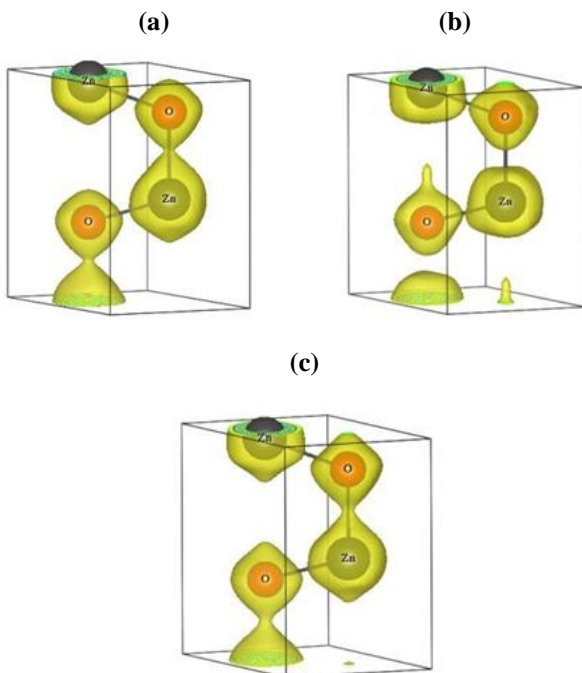


Fig. 4. 3D unit cell of Zn_{1-x}Co_xO materials, a) x=0.0, b) x=0.04, c) x=0.06.

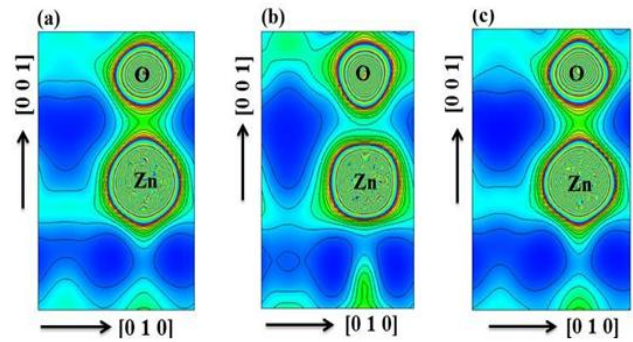


Fig. 5. 2D ED maps on (100) lattice plane of Zn_{1-x}Co_xO materials, a) x=0.0, b) x=0.04, c) x=0.06.

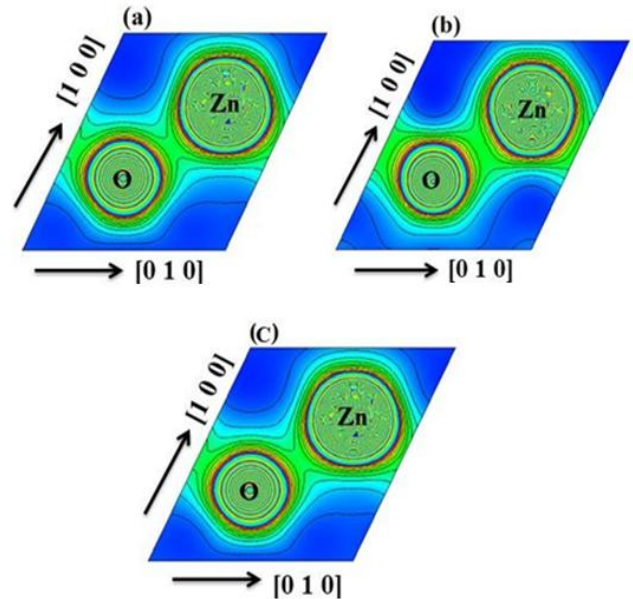
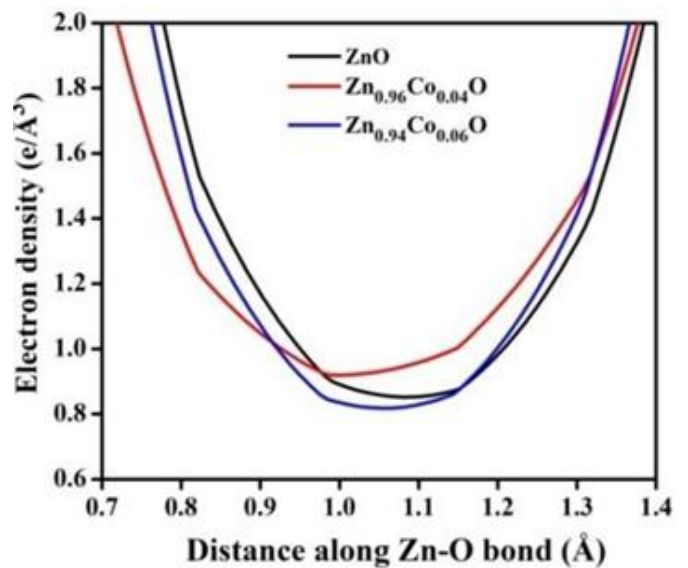


Fig. 6. 2D ED maps on (103) lattice plane of Zn_{1-x}Co_xO materials, a) x=0.0, b) x=0.04, c) x=0.06.



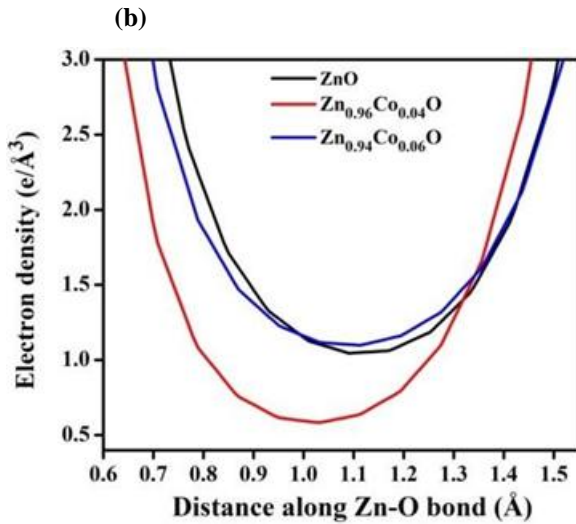


Fig. 7. 1D ED profiles of Zn_{1-x}Co_xO materials a) Bond 1, b) Bond 2

TABLE II. BONDING BEHAVIOR OF Zn_{1-x}Co_xO

Nominal Co concentration (mol %)	Bond 1		Bond 2	
	Distance of Zn-O bond	Mid bond electron density (e/Å ³)	Distance of Zn-O bond	Mid bond electron density (e/Å ³)
x=0.0	1.9741	0.8522	1.9919	1.0451
x=0.04	1.9704	0.9190	2.0136	0.5834
x=0.06	1.9720	0.8180	2.0127	1.1008

IV. CONCLUSION

Cobalt doped zinc oxide (Zn_{1-x}Co_xO (x = 0.0, 0.04 and 0.06)) materials were synthesized using solid state sintering process by means of microwave medium. PXRD profiles confirm that the prepared systems with phase pure ZnO. The detailed structural information of prepared system was investigated by Rietveld profile refinement technique. The difference of morphologies between pure and cobalt doped ZnO samples were found in SEM measurements. Charge density distribution analyses have done in maximum entropy method and charge derived properties are consistent with PXRD data.

ACKNOWLEDGMENT

One of author D.S acknowledges the management of Kalasalingam Academy of Research and Education (KARE) for offering fellowships (URF). Authors acknowledge International Research Centre (IRC), KARE for supporting instrumentation facilities..

REFERENCES

1. T. Guo, M.S. Yao, Y.H. Lin, & C.W.A. Nan, comprehensive review on synthesis methods for transition-metal oxide nanostructures. *Cryst Eng Comm*, 17(19), pp. 3551–3585 (2015).
2. A.B. Djurišić, X. Chen., Y.H. Leung., & A. Man Ching Ng. ZnO nanostructures: Growth, properties and applications. *Journal of Materials Chemistry*, 22(14), pp.6526–6535 (2012).
3. R. Brayner., S.A. Dahoumane., C. Yéprémian., C. Djediat., M. Meyer., A. Couté., & F. Fiévet. ZnO nanoparticles: Synthesis, characterization, and ecotoxicological studies. *Langmuir*, 26(9), pp.6522–6528 (2010).
4. K. U-Thaipan & K. Tedsree. Manipulation of surface morphology of flower-like Ag/ZnO nanorods to enhance photocatalytic performance. *Advances in Natural Sciences: Nanoscience and Nanotechnology*, 9(2). (2018).

5. R. Habibi., A.M. Rashidi., J.T. Daryan., & A.M.A. Zadeh. Study of the Rod-Like and spherical nano-ZnO morphology on H₂S removal from natural gas. *Applied Surface Science*, 257(2), pp.434–439 (2010).
6. K.H. Kim, Y. Yoshihara, Y. Abe, M. Kawamura, & T. Kiba, Morphological characterization of sphere-like structured ZnO-NiO nanocomposites with annealing temperatures. *Materials Letters*, 186 (October 2016), pp.364–367 (2017).
7. C. Liewhiran, & S. Phanichphant, Influence of thickness on ethanol sensing characteristics of doctor-bladed thick film from flame-made ZnO nanoparticles. *Sensors*, 7(2), pp.185–201 (2007).
8. M. Pudukudy, & Z. Yaakob, Facile solid state synthesis of ZnO hexagonal nanogranules with excellent photocatalytic activity. *Applied Surface Science*, 292, pp.520–530 (2014).
9. S.Y. Purwaningsih, S. Pratapa, Triwikantoro, & Darminto. Synthesis of nano-sized ZnO particles by co-precipitation method with variation of heating time. *AIP Conference Proceedings*, 1710 (2016).
10. J.N. Hasnidawani H.N. Azlina., H. Norita, & N.N. Bonnia, S. Ratim & E.S. Ali, Synthesis of ZnO Nanostructures Using Sol-Gel Method. *Procedia Chemistry*, 19, 211–216 (2016).
11. Z. Cao, Y. Wang, Z. Li, & N. Yu, Hydrothermal Synthesis of ZnO Structures Formed by High-Aspect-Ratio Nanowires for Acetone Detection. *Nanoscale Research Letters*, 11(1), pp.4–9 (2016).
12. Z. Chen, K. Shum, Salagaj, T., Zhang, W., & Strobl, K. ZnO thin films synthesized by chemical vapor deposition. 2010 Long Island Systems, Applications and Technology Conference, LISAT 10, pp.4–9 (2010).
13. K. Anand, S. Varghese, & T. Kurian, Effect of ball size on milling efficiency of zinc oxide dispersions. *Particulate Science and Technology*, 36(3), pp.308–311 (2018).
14. K. Tahmasebi, M. Maleki Shahraki, & T. Ebadzadeh, Effect of microwave sintering on the microstructure and electrical properties of low-voltage ZnO varistors. *Materials and Manufacturing Processes*, 33(8), pp.817–821 (2018).
15. R.F.K. Gunnewiek, & R.H.G.A. Kiminami, Two-step microwave sintering of nanostructured ZnO-based varistors. *Ceramics International*, 43(1), pp.847–853 (2017).
16. R.F.K. Gunnewiek, & R.H.G.A. Kiminami, Effect of heating rate on microwave sintering of nanocrystalline zinc oxide. *Ceramics International*, 40(7 PART B), pp.10667–10675 (2014).
17. D. Sivaganesh, S. Saravanakumar, V. Sivakumar, K.S.S Ali, E. Akapo, E. Alemayehu, R. Saravanan, Structural, optical and charge density analysis of Al doped ZnO Materials. *Journal of Materials Science: Materials in Electronics*, 30(3), pp.2966–2974 (2019).
18. International Centre of Diffraction Data, Powder Diffraction File, JCPDS File No 00-036-1451, (1996).
19. S. Saravanakumar, J. Kamalaveni, M.P. Rani, & R. Saravanan, Solubility of Mn stabilized cubic Zirconia nanostructures. pp.837–843 (2014).
20. A.L. Patterson, The Scherrer Formula for I-Ray Particle Size Determination. *Phys. Rev.*, 6, pp.978–982 (1939).
21. V. Petricek, M. Dusek, L. Palatinus, Jana2006. The crystallographic computing system, Institute of Physics, Praha, Czech Republic, (2006). vol. 2012, 604241, pp 1-11, 2012. <https://doi.org/10.5402/2012/604241>.
22. N. Wu, *The Maximum Entropy Method* (Springer), Berlin Heidelberg, pp.1–334, (1997).
23. K. Momma, T. Ikeda, A.A. Belik, F. Izumi, Dysnomia, A computer program for maximum-entropy method (MEM) analysis and its performance in the MEM-based pattern fitting, pp.1–10, (2013).
24. K. Momma, F. Izumi, VESTA 3 for three-dimensional visualization of crystal, volumetric and morphology data, pp.1272–1276 (2011).

AUTHORS PROFILE



D. Sivaganesh is a Ph.D student at Kalasalingam University, India. His research interest is structural and photoluminescence properties of phosphor materials.





S. Sasikumar received his Ph.D degree in 2018 at Madurai Kamaraj University, India. His research interest is the applications of piezo – electric materials. He has published 19 research articles in reputed journal with 56 citations



S. Saravanakumar is working as an assistant professor at Kalasalingam University and he received his Ph.D. degree in 2015 at Madurai Kamaraj University, India. His main research interest is materials science. He has published 26 articles in journals with over 107 citations



S. Asath Bahadur is working as professor at Kalasalingam University, India. His research interest is in the field of single crystal material for non – linear optical application.